RSC Advances

PAPER

View Article Online
View Journal | View Issue

Cite this: *RSC Adv.*, 2022, **12**, 14698

5-*N*-Arylaminothiazoles with pyridyl groups and their first-row transition metal complexes: synthesis, photophysical properties, and Zn sensing†

Khurnia Krisna Puji Pamungkas, Toshifumi Maruyama and Toshiaki Murai *

A series of 5-*N*-arylaminothiazoles were synthesized with facile diversity-oriented synthesis from readily available starting materials *via* the reaction of thioamide dianions and thioformamides. The introduction of various substituents at the 2-position of a thiazole ring (*i.e.*, 2-pyridyl, 4-methylpyridyl, and phenyl groups) and on the nitrogen atom (*i.e.*, *p*-tolyl and phenyl groups) significantly influenced the absorption and emission spectra of the isolated compounds. X-ray analysis confirmed that the substituents at the amino site were twisted from a thiazole ring, while the formation of its nickel complex showed dinuclear metal complexes bridged with chlorine atoms. Moreover, the formation of zinc–thiazole complexes showed enhanced emission properties in solution and noticeable emission in a solid state. In addition, thiazole-bridged dypyrromethene type ligands showed high selectivity toward Zn^{+2}, which make them good candidates for zinc sensing.

Received 16th March 2022
Accepted 9th May 2022

DOI: 10.1039/d2ra01694j

rsc.li/rsc-advances

Introduction

Thiazoles are five-membered heteroaromatics that contain sulfur and nitrogen atoms in a cyclic ring system (Fig. 1). One of the distinctive features of thiazoles is that they have a sulfur atom, which is a soft base, and a nitrogen atom, which is a hard base. This implies that thiazoles can coordinate to a range of soft and hard metals. Moreover, the calculated π-electron densities of thiazoles suggest that C_5 is the most favorable site for electrophilic substitutions, followed by C_4, while C_2 is a preferable site for nucleophilic substitutions.[1]

Many thiazole-based compounds are now in clinical use, such as the anticancer drug dasatinib,[2] and the anti-HIV drug ritonavir.[3] Additionally, thiazoles have three carbon atoms at the 2-, 4-, and 5-positions, to which a wide variety of substituents can be principally introduced. Therefore, a wide range of thiazole derivatives have been developed. On the other hand, the chemistry of thiazoles has been extended to the development of thiazole-based fluorescent materials. These fluorescent compounds exhibit unique photophysical properties such as aggregation induced emission (AIE),[4,5] thermochromism,[4] mechanochromism,[6] and large Stokes shifts,[7] and some of them are acid-responsive fluorescent compounds (Fig. 2).[8]

Thiazole can connect to several electron donor-containing fragments which exhibit coordination ability such as a pyridyl group. Due to this modification, several thiazoles coordinated to a boron atom have been reported to show acid-responsive properties[9] and aggregation induced emission (AIE) with high quantum yields of up to 95% in the solid state.[10] Moreover, thiazoles are also suitable as organic ligands to various metal. In fact, the presence of a metal surface closest to the fluorescent molecule can manipulate the decay rate of the fluorophore and produce drastic spectral changes.[11] Moreover, interactions

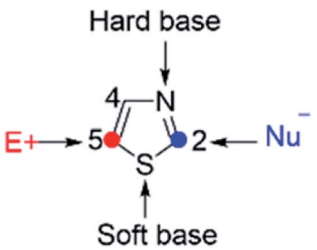

Fig. 1 Thiazole structure.

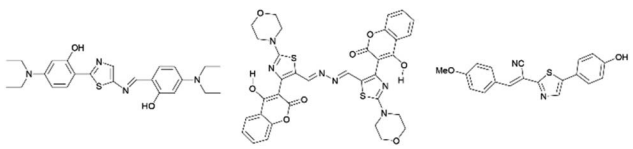

Fig. 2 Selected examples of thiazole fluorescent compounds.

Department of Chemistry and Biomolecular Science, Faculty of Engineering, Gifu University, Yanagido, Gifu 501-1193, Japan. E-mail: mtoshi@gifu-u.ac.jp

† Electronic supplementary information (ESI) available. CCDC 2155547 and 2155549. For ESI and crystallographic data in CIF or other electronic format see https://doi.org/10.1039/d2ra01694j

between a metallic surface with fluorophores have a beneficial effect on photophysical properties such as an increased quantum yield, improved photostability and a reduced lifetime of fluorophores.[12]

Intense studies on thiazole-based ligands coordinated to a transition metal have increased over the past several years. A considerable number of metal–thiazole complexes have been discovered to be catalytically[13,14] and biologically active compounds for medical applications.[15,16] In addition, the most commonly reported thiazoles coordinated to transition metals that show luminescence properties are complexes with ruthenium,[17–19] iridium,[20] rhenium,[21] platinum,[22] and lanthanoid elements (Fig. 3).[23–25]

Those works have mainly focused on the second- and third-row transition metals, while the uses of the first-row transition metals (Fe, Co, Ni, Co, and Zn) are less favorable due to their exceptionally short CT lifetimes arising from deactivation through low-lying ligand-field excited states.[26] Nevertheless, the coexistence of nitrogen and sulfur atoms in a thiazole ring could promote the stabilization of Ni(II) complexes.[27] Some of the first-row transition metals such as nickel and zinc are widely used as complexing agents for various purposes. For example, zinc metal complexes with thiazole pyridine-based ligands are biologically active as anti-microbial and anti-tumor agents.[16] Meanwhile, nickel coordinated to thiazole-4-carboxylic acid exhibited polymorphism properties.[28] However, there have been only a few reports on first-row transition metal–thiazole complexes.[29,30] (Fig. 4).

Recently, several fluorescent molecules have been used for the molecular recognition of zinc ions. However, due to its closed shell electron configuration ($3d^{10}$), zinc ion is silent with respect to spectroscopic or magnetic signals.[31,32] Therefore, a reliable technique for the detection of zinc ion is highly desirable. The most promising method for detecting zinc ion is by using fluorescence. Besides, fluorescence detection is fast, efficient, and simple.[33,34] For example, imidazole-based compounds showed an increase in emission intensity in the presence of zinc ions.[35] Meanwhile, zinc sensing based on thiazole compounds showed turn on–off emission properties[36] and a strong emission response and a high quantum yield on addition of zinc ions (Fig. 5).[37]

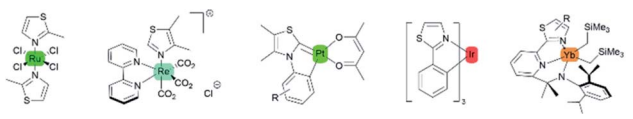

Fig. 3 Selected examples of transition metal–thiazole complexes.

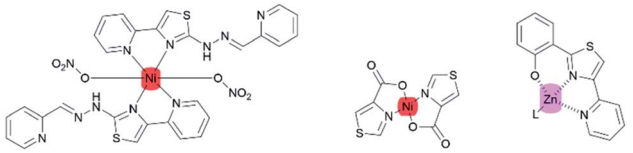

Fig. 4 First-transition thiazole metal complexes.

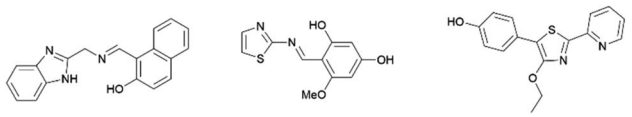

Fig. 5 Fluorescent molecules for zinc sensing.

Our group has been interested in the chemistry of 5-*N*-arylaminothizoles for many years. Therefore, a considerable number of these compounds have been developed.[38–44] 5-*N*-Arylaminothiazoles are a class of fluorescent compounds bearing a flexible conformational geometry with non-planar carbon skeletons.[38] These compounds are synthesized by reacting secondary thioamide and thioformamides *via* thioamide dianions and thiazolines. This synthetic protocol allows us to access a wide range of unprecedented 5-*N*-arylaminothiazoles with various substituents at the 2- and 4-positions of a thiazole ring.

Herein we report a series of 5-*N*-arylaminothiazole having pyridyl groups and their first-row transition metal complexes. The synthesis, structural elucidation, and photophysical properties both in a solid state and in solution are discussed.

Results and discussion

Synthesis of 5-aminothiazolines and 5-*N*-arylaminothiazoles

The synthesis of ligands is depicted in Scheme 1. The new thiazole ligands were synthesized by deprotonation of secondary thioamides **1** with 2 equivalents of organolithium (*n*-BuLi) at low temperature to generate thioamide dianions **1a**. Addition of thioformamides **2** and iodine to the reaction mixture gave 5-aminothiazolines **3** as major products.[44] Further oxidation of 5-aminothiazolines **3** with 2 equivalents of iodine resulted in the formation of the corresponding 5-aminothiazole ligand **4** in low to good yields. Following this reaction, a wide range of substituents possessing electron-donating and -withdrawing properties could be introduced to the 2-, 4-, and 5-positions of the thiazole ring.

As a result, the introduction of pyridyl groups at the 2- and 4-positions gave **4a** in 23% yield. Replacement of a methyl group with other functional groups at the 5-position of a thiazole ring led to an increase in the yield of the product. Incorporation of a tolyl group significantly improved the yield of the product **4b** to 58%. In addition, the introduction of a methyl group at the

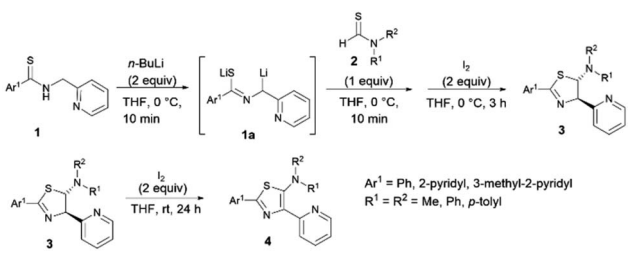

Scheme 1 Synthesis of 5-aminothiazolines and 5-*N*-arylaminothiazoles.

para position of a pyridyl moiety gave **4c** in 57% yield. Furthermore, the incorporation of pyridyl groups only at the 2- or 4-positions of a thiazole ring afforded thiazole products **4d**, **4e**, and **4f** in yields of 59%, 82% and 90%, respectively (Fig. 6).

In addition, we also synthesized dipyrromethene-type ligands **6** following the protocol reported previously by our group.[9] Initially, the 5-H thiazoles **5** undergo bromination reaction followed by Buchwald–Hartwig amination to give the corresponding thiazole ligands **6a** and **6b** in yields of 60% and 49%, respectively (Scheme 2).

Synthesis of first-row transition metal–thiazole complexes

A series of nickel–thiazole complexes **7** were prepared in two steps: (i) reflux of the metal source in ethanol under an inert atmosphere, (ii) synthesis of the desired final products by reacting the corresponding ligand **4** with nickel chlorides under reflux. As a result, all of the metal complexes were isolated in moderate to high yields (Fig. 7). ESI-mass analysis suggested two sets of nickel complex formations such as $[Ni(L)X_2]$ for nickel complex having a tridentate ligand (**7a**, **7b**, and **7c**) and $[Ni(L_2)X_2]$ for nickel complex having a bidentate ligand (**7d**, **7e**, and **7f**).

Having succeeded in the synthesis of nickel–thiazole complexes, we then turned our attention to the synthesis of metal–thiazole complexes using other first-row transition metal atoms such as zinc. A series of zinc–thiazole metal complexes were synthesized by simply mixing the corresponding thiazoles **4f** with zinc halides at room temperature. Following this procedure, new zinc thiazole complexes **7** with different halides were synthesized in moderate to high yields (Fig. 8). To our delight, these complexes showed good solubility in most organic solvents. ESI-mass analysis suggested that the zinc atom is coordinated to two bidentate thiazole ligands to form 2 : 1 metal complexes $[Zn(L_2)X_2]$.[44]

Solutions of these zinc complexes in deuterated chloroform were prepared for NMR analyses. With the addition of 1 equivalent of zinc ion, the signals of protons of the thiazole ligand at 8.57 ppm and 7.83 ppm were shifted downfield to at 8.75 ppm and 8.04 ppm, respectively. Furthermore, in the formation of zinc complexes, two new doublet peaks integrated for 8 protons assigned to phenyl rings in the tolyl groups appeared at 7.00 ppm and 6.90 ppm, respectively. However, the proton signal and chemical shift of the complexes are almost identical despite having different halogens at the zinc center (Fig. 9). These results indicate the zinc–thiazole complexes **8** are formed on the addition of zinc halides.

X-ray crystallography analyses

High-quality single green crystals of thiazoles **4c** were isolated in the triclinic space group $P\bar{1}$ (Fig. 10). X-ray crystallography of

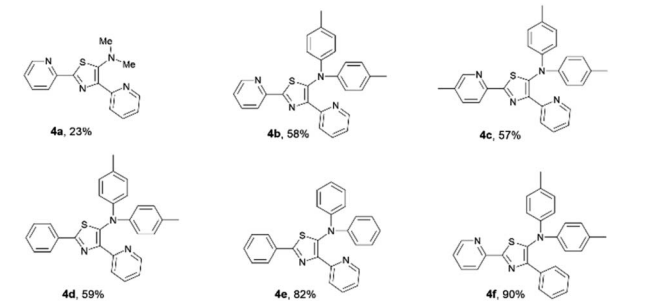

Fig. 6 A series of isolated 5-*N*-arylaminothiazoles.

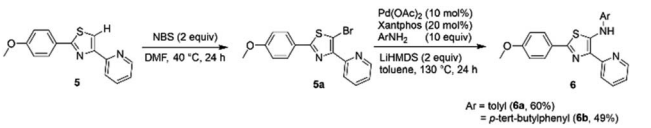

Scheme 2 Synthesis of dipyrromethene-type ligands **6**.

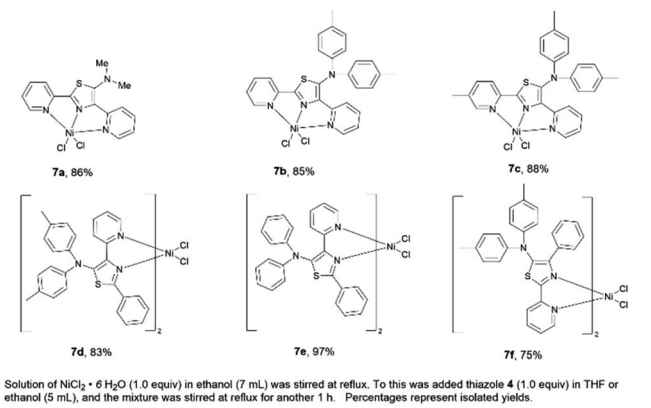

Fig. 7 A series of isolated nickel–thiazole complexes.

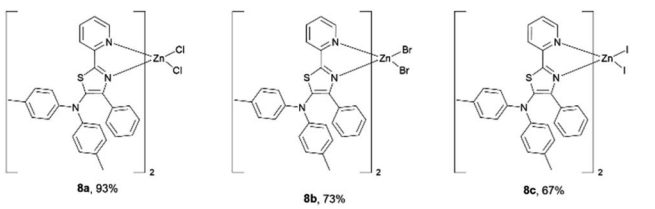

Fig. 8 A series of isolated zinc–thiazole complexes.

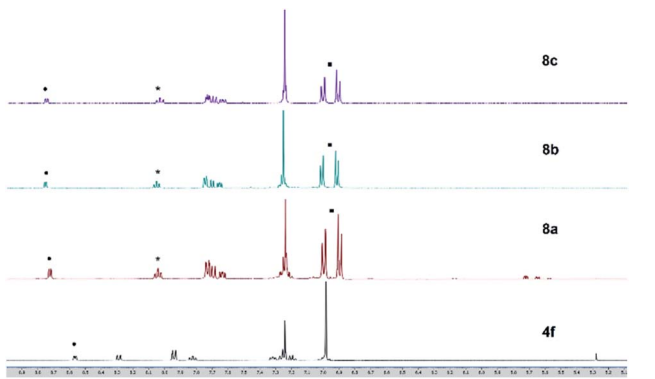

Fig. 9 ^{1}H NMR (500 MHz, $CDCl_3$) charts of ligand **4f** and zinc thiazole complexes **6a–c**.

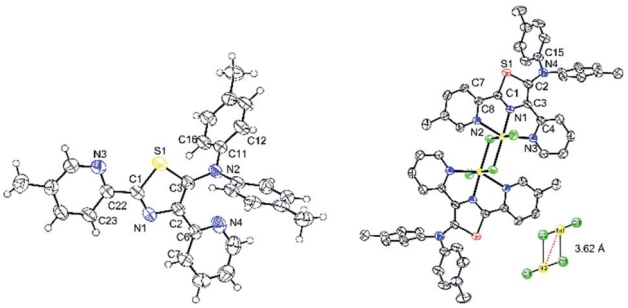

Fig. 10 X-ray structure of thiazole **4c** (left) and nickel–thiazole complex **7c** (right). Hydrogen atoms are omitted for clarity.

4c confirmed the twisted conformation geometry of amino groups at the 5-position of a thiazole ring with torsion of 108.0° (S1–C3–N2–C11). Meanwhile, two pyridyl groups attached at the thiazole ring were located almost in the same plane as the thiazole ring. Moreover, a green crystal of **7c** showed the formation of dinuclear nickel complexes with a *trans* configuration in a distorted octahedral geometry (Fig. 9). Two bridging Cl atoms connect two central nickel atoms between two dimers with a distance of 3.620 Å between Ni1–Ni2 (inset: Fig. 10). The distance of bridging Ni1–Cl2 was 2.600 Å, which is longer than that of Ni1–Cl3 2.363 Å. The atoms Cl1–Ni1–Cl2 were oriented almost linearly with a bond angle of 177.55 (4)°, while the atoms Cl2–Ni1–N2 were oriented almost perpendicularly with a bond angle of 89.15°. The torsion angle of the amino groups in complex **7c** (S1–C2–N4–C15) were 43.31°. Moreover, the distances of Ni1–N1 (thiazole ring) and Ni1–N3 (pyridyl group) was found to be 1.970 and 2.198 Å, respectively.

Photophysical properties of 5-*N*-arylaminothiazoles and their complexes in solution

The absorption and emission spectra of isolated 5-aminothiazole derivatives in chloroform are shown in Fig. 11 and Table 1. The absorption maxima range from 349 to 398 nm. That of thiazole **4a** was in the shortest absorption region, and gradually shifted to longer wavelengths with introduction of a tolyl group to the nitrogen atom at the 5-position of a thiazole ring, such as **4b**. Interestingly, the incorporation of a methyl group at the *para* position of a pyridyl group slightly shifted the absorption maxima to a shorter wavelength, such as in **4c**. Further blue-shift absorption was observed by replacing a tolyl group with a phenyl group at the 2-position of the thiazole ring

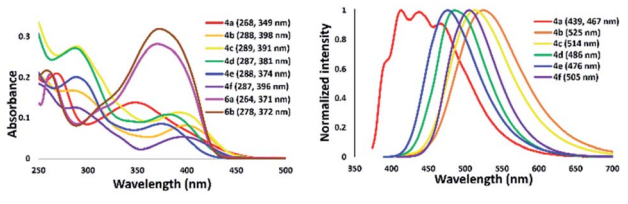

Fig. 11 Absorption (right) and emission spectra of 5-*N*-arylaminothiazoles in chloroform [10^{-5} M].

Table 1 Spectroscopic data of a series of 5-*N*-arylaminothiazoles[a]

Thiazole	λ_{abs} (nm)	log ε	λ_{ex} (nm)	λ_{em}[b] (nm)	ν_{ss} [cm^{-1}] (nm)	φ_F[c]
4a	349	4.14	359	467	[7240] (118)	0.04
4b	398	3.90	397	525	[60781] (127)	0.13
4c	391	4.05	395	514	[61201] (123)	0.16
4d	381	4.03	377	486	[56701] (113)	0.2
4e	374	3.92	376	476	[5729] (102)	0.31
4f	396	3.72	392	505	[5450] (109)	0.42
6a	371	4.44	—	—	—	—
6b	372	4.50	—	—	—	—

[a] In chloroform [conc. = 10^{-5} M]. [b] Excited in λ_{max}. [c] Absolute quantum yield of fluorescence.

of **4d**. In addition, when a phenyl group was placed at the 2-position and the nitrogen atom at the 5-position of a thiazole ring for **4e**, the absorption maxima shifted to 374 nm, while the introduction of a phenyl group at the 4-position of a thiazole ring for **4f** shifted the absorption maxima to 396 nm. Furthermore, the emission maxima of 5-*N*-arylaminothiazoles varied from 467–525 nm depending on the substituents. These results showed that the photophysical properties of 5-*N*-arylaminothiazoles could be finely tuned simply by introducing different substituents at the thiazole ring. In addition, the emission maxima of **6a** and **6b** were observed at 371 nm and 372 nm, respectively. However, these dipyrromethene-type ligands did not show emission properties.

We next examined the spectroscopic properties of nickel–thiazole complexes **7** in dilute chloroform (Fig. 12 and Table 2). The longest absorption spectra of nickel complexes **5** ranged from 278 to 424 nm. The absorption maxima of **7a** were observed at 388 nm and were significantly red-shifted for

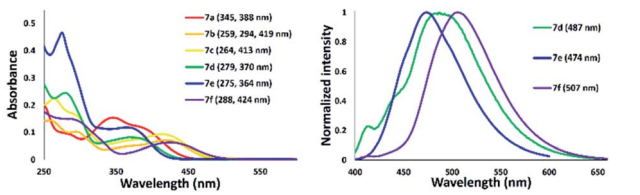

Fig. 12 Absorption (right) and emission spectra of nickel–thiazole complexes in chloroform [10^{-5} M].

Table 2 Spectroscopic data of nickel–thiazole complexes[a]

Thiazole	λ_{abs} (nm)	log ε	λ_{ex} (nm)	λ_{em}[b] (nm)	ν_{ss} [cm^{-1}] (nm)	φ_F[c]
7a	388	4.06	359	—	—	—
7b	419	3.85	397	—	—	—
7c	413	3 96	395	—	—	—
7d	370	3.91	377	487	[6493] (117)	0.04
7e	364	4.07	376	474	[6375] (110)	0.03
7f	424	3.79	392	507	[3861] (83)	0.02

[a] In chloroform [conc. = 10^{-5} M]. [b] Excited in λ_{max}. [c] Absolute quantum yield of fluorescence.

a thiazole complex having a tolyl group on the nitrogen atom at the 5-position of a thiazole ring such as **7b**. The presence of a methyl group at the *para* position of the pyridyl group slightly shifted the absorption maxima to a shorter wavelength of **7c**. The absorption maxima of **7d** were blue-shifted to 370 nm with the introduction of a phenyl substituent at the 2-position of a thiazole ring. Meanwhile, replacement of a tolyl group by adding a phenyl group at the 2-position and on the nitrogen atom attached to a thiazole ring shifted the absorption maxima to 364 nm, such as in **7e**. Moreover, a nickel–thiazole complex having a phenyl group at the 4-position instead of pyridyl and tolyl groups on the nitrogen atom **7f** was observed at 424 nm. In addition, the formation of a nickel–thiazole complex turned the emission properties off, as in **7a**, **7b**, and **7c**. No emission was observed in either in a solid state or in solution. In contrast, the formation of nickel complexes **7d**, **7e** and **7f** had no effect on emission, and they are still emissive in a solution to some extent under UV illumination.

The photophysical properties of a series of zinc–thiazole complexes investigated in a THF solution are shown in Fig. 13. The absorption maxima of zinc complexes **8a–c** in THF were observed at 390 nm in all cases, while that of zinc thiazole having an iodine **8c** was slightly blue-shifted to 384 nm. Meanwhile, their emission maxima showed no significant change even when we introduced different halogens on the zinc center. Interestingly, zinc–thiazole complex containing a bromide **8b** showed a high quantum yield of up to 75%. Fluorescence lifetime decay of thiazole ligand **4f** and zinc-complexes **8** in THF was in the range 4.43–4.94 ns. The thiazole **4f** exhibited fluorescence lifetimes about 4.93 ns. Introduction of dichloride and zinc dibromide to the zinc center shortened the fluorescence lifetime such as **8a** and **8b**. Interestingly, zinc–thiazole complex having an iodine atom in the metal center **8c** possessed the longest average fluorescence lifetimes (Table 3).

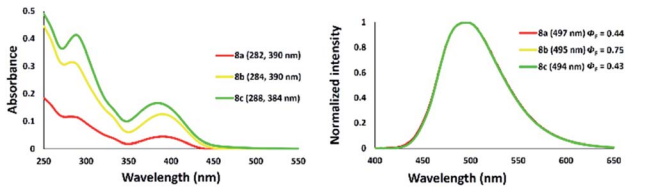

Fig. 13 Absorption (right) and emission spectra of zinc–thiazole complexes **8a–c** in THF [10^{-5} M].

Solvatochromism properties of 5-*N*-arylaminothiazoles and their complexes

The emission color of the isolated 5-*N*-arylaminothiazoles varied with the solution polarity exhibited a tunable emission wavelength in the range of 397–505 nm.[44] The emission maxima of **4f** strongly depended on the solvent polarity, and thus their peak emissions were greatly affected. Large red shifts in the emission maxima (Fig. 14) were observed upon changing from a nonpolar (cyclohexane) to a polar (MeOH) solvent and cover blue to green color with low quantum yield. In addition, zinc–thiazole complex **8a** also showed solvatochromism properties and transitioned from a blue to green color. Uniquely, the emission maxima of **8a** in halogenated solvents (dichloromethane and chloroform) were more red-shifted compared to its emission maxima in non-halogenated (THF and MeOH) solvents (Fig. 14). To our delight, zinc–thiazole complex **8a** showed comparable quantum yields with the free ligand **4f**.

Photophysical properties of 5-*N*-arylaminothiazoles and their complexes in a solid state

In addition to showing bright emission in solution, 5-*N*-arylaminothiazoles **4** and their zinc–thiazole complexes **8** also exhibited emission in a solid state. However, thiazole **4a** and the formation of nickel–thiazole complexes **7** did not show any noticeable emission properties in a solid state. Thiazoles **4b–f** showed emission in a solid state with a quantum yield (φ_F) reaching up to 52%. The absorption maxima of **4b–d** were observed in almost the same absorption region, while of those **4e** and **4f** were slightly blue-shifted to 427 nm and 404 nm, respectively. Their longest emission maxima appeared from 469 nm to 542 nm with low to moderate quantum yields.

The absorption and emission maxima of zinc–thiazole complexes **8** in a solid state were significantly different than those of the free ligands (Table 4). While the longest absorption maxima ranged from 440 nm to 452 nm, while their emission maxima varied depending on the halogens on the zinc center. The zinc thiazole complex with chlorine atoms at the zinc center **8a** showed a significant red-shift to 611 nm compared to that of the free ligand **4f** at 475 nm. Furthermore, the introduction of bromine (**8b**) and iodine atoms (**8c**) to the zinc center shifted the emission maxima to a shorter emission wavelength at 550 nm and 548 nm, respectively. The emission decay analysis showed significant decreasing of fluorescence lifetimes of zinc–thiazole complexes **8** compared to its free ligand **4f** (Table 4). Moreover, the quantum yield of the complexes dropped

Table 3 Spectroscopic data of 5-*N*-arylaminothiazole **4f** and zinc–thiazole complexes in THF [10^{-5} M][a]

Thiazole	λ_{abs} (nm)	log ε	λ_{ex} (nm)	λ_{em}[b] (nm)	ν_{ss} [cm^{-1}] (nm)	φ_F[c]	χ^{2}[d]	τ[d] (ns)
4f	390	3.92	385	495	[5504] (105)	0.5	1.8	4.93
8a	390	3.64	384	497	[5520] (107)	0.4	2.7	4.86
8b	390	4.1	384	495	[5504] (105)	0.8	2.1	4.43
8c	384	4.22	386	494	[5798] (110)	0.4	2	4.94

[a] Measured in THF. [b] Excited in λ_{max}. [c] Absolute quantum yield of fluorescence. [d] Excited at 365 nm.

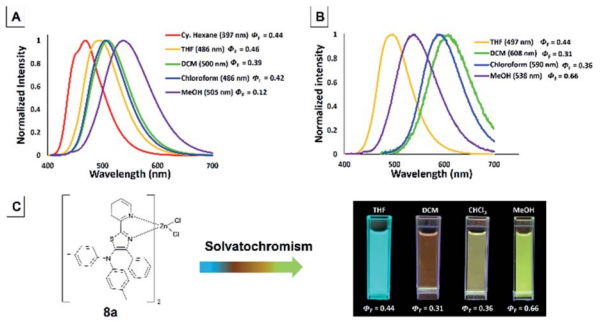

Fig. 14 Emission spectra of 5-aminothiazole **4f** (A) and zinc–thiazole complex **8a** (B) [10^{-5} M]. Change in the color of emission for **8a** in solvent with different polarities (C).

Table 4 Spectroscopic data of 5-*N*-arylaminothiazoles and zinc–thiazole complexes in a solid state

Thiazole	λ_{abs} (nm)	λ_{ex} (nm)	$\lambda_{em}{}^{a}$ (nm)	ν_{ss} [cm^{-1}] (nm)	$\varphi_F{}^{b}$	χ^{2c}	τ^{c} (ns)
4b	442	439	495	[2411] (53)	0.21	1.66	2.53
4c	444	437	542	[3438] (80)	0.06	3.5	2.47
4d	444	437	475	[1469] (31)	0.21	1.56	2.77
4e	427	428	469	[2097] (42)	0.15	1.36	1.91
41	404	431	475	[3609] (71)	0.52	1.54	3.03
8a	440	370	611	[6360] (171)	0.02	3.21	121
8b	440	365	550	[4545] (110)	0.05	2.41	1.99
8c	452	492	548	[3875] (96)	0.02	2.66	0.23

[a] Excited in λ_{max}. [b] Absolute fluorescence of quantum yield. [c] Excited at 365 nm.

significantly in a solid state. However, the difference in emission color under UV irradiation at 365 nm was still easily visible with the naked eye (Fig. 15).

Use of 5-*N*-arylaminothiazoles as a fluorescence probe for detection of zinc ion

Coordination of Zn^{2+} with dipyrromethene-type ligands **6** turned on the emission properties for **6b**. Considering this unexpected result, we then investigated the possibility of using **6b** for Zn^{2+} sensing. We initially titrated of various metal cations such as Cu^{2+}, Ca^{2+}, Fe^{3+}, and Zn^{2+} into a THF solution of dipyrromethene-type ligand **6b**. As a result, compound **6b** showed high selectivity for Zn^{2+} ions. With the

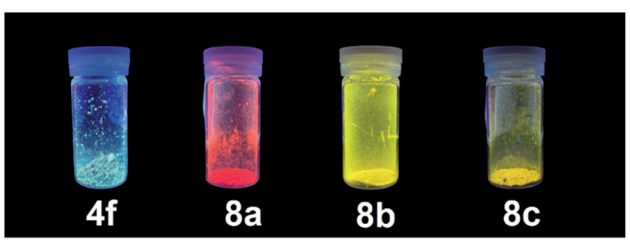

Fig. 15 Emission color in a solid state of 5-aminothiazole **4f** and zinc–thiazole complexes **8a–c** under UV radiation at 365 nm.

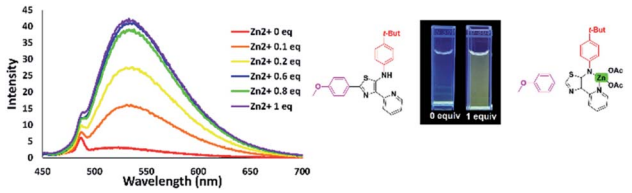

Fig. 16 Fluorescence titration of **6b** with different amounts of zinc ions in THF solution [10^{-5} M].

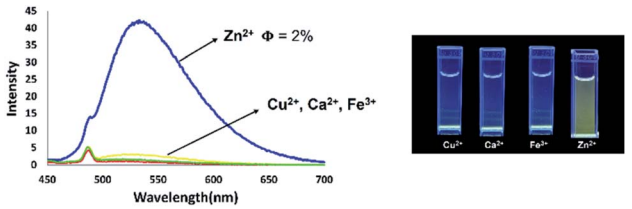

Fig. 17 Fluorescence titration of **6b** with different cations in THF solution [10^{-5} M].

addition of Zn^{2+}, the emission intensity at 533 nm continued to increase with the appearance of a green emission with a low quantum yield (φ_F) of 0.02 under UV irradiation at 365 nm (Fig. 16).

In contrast, the emission properties of **6b** towards cations other than Zn^{2+} did not show any change in emission intensity even after the addition of 1 equivalent of cation. These results imply that **6b** has excellent potential as a candidate for Zn^{2+} fluorescence sensing (Fig. 17).

Conclusions

In summary, a series of 5-*N*-arylaminothiazole derivatives having pyridyl groups were successfully synthesized and systematically characterized. The absorption and emission properties of isolated 5-*N*-arylaminothiazoles were finely tuned simply by varying the substituents attached to the thiazole ring and the nitrogen atom at the 5-position. The longest absorption spectra ranged from 349 to 396 nm. They also showed solvatochromism properties in solvent with different solvent polarities. X-ray analyses revealed that the isolated 5-*N*-arylaminothiazole adopts a highly twisted conformation, wherein the diarylamino group deviates from the thiazole ring. The crystal structure of nickel–thiazole complex **7c** confirmed the formation of dinuclear metal complexes with chlorine atom acting as a bridge between two nickel complexes. However, the formation of nickel complexes turned off the emission properties of some complexes. In contrast, the formation of zinc–thiazole complexes showed emission both in solution and in a solid state. Moreover, dipyrromethene-type ligands showed consistent enhancement of emission intensity upon the addition of Zn^{2+}. Therefore, these ligands can be used for zinc sensing. Further applications of 5-*N*-arylaminothiazoles as chemosensors and biosensors will be reported in due course.

Experimental section

General procedure A: preparation of thiazoles

To a solution of thiazolines (1 equiv.) in THF was added iodine (2 equiv.) at room temperature, and the mixture was stirred for 24 h. The resulting mixture was poured into a saturated aqueous solution of $Na_2S_2O_3$ and extracted with Et_2O. The organic layer was dried over $MgSO_4$ and concentrated *in vacuo*. The residue was purified by column chromatography (SiO_2) to give the corresponding thiazoles.

General procedure B: preparation of dipyrromethene type ligands

$Pd(OAc)_2$ (10 mol%) and xantphos (20 mol%) were weighted into Schlenk tube that was sealed with a septum and purged with argon (3 times). Toluene (6 mL) then injected, and the reaction was continued for 15 min at 130 °C. 5-Bromothiazole (1 equiv.) in 4 mL toluene was then injected *via* syringe followed by the amine (10 equiv.) and LiHMDS (2 equiv.). The reaction mixture was filtered through a bed of Celite and washed with CH_2Cl_2. The filtrate was concentrated *in vacuo* and purified *via* silica gel flash column chromatography (SiO_2, hexane : EtOAc) to give the corresponding thiazoles.

General procedure C: preparation of nickel thiazole complexes

$NiCl_2 \cdot 6H_2O$ (1 equiv.) was taken in ethanol and was heated to reflux. The 5-*N*-arylaminothiazoles (1 equiv.) in a EtOH solution was added dropwise to the refluxing solution and was further refluxed for another 1 h. The final mixture was concentrated *in vacuo*. The obtained participate product was then washed by ethanol and diethyl ether. To give pure nickel–thiazole complexes.

General procedure D: preparation of zinc thiazole complexes

To a solution of thiazoles (1 equiv.) in THF was added zinc halides (1 equiv.) at room temperature, and the mixture was stirred for 24 h. The precipitate was then washed with hexane and Et_2O to give pure zinc–thiazole complexes.

Fluorescence lifetime analysis

All zinc complexes were analyzed in dilute THF [10^{-5} M] using the Fluorescence Lifetime Spectrometer Quantaurus-Tau® C16361 Series with a measurement time range of 50 ns and frequencies at 5 MHz.

N,*N*-Dimethyl-2,4-di(pyridin-2-yl)thiazol-5-amine (4a)

General procedure A. 4a (0.193 g, 23%) as a yellow solid (mp: 64–65 °C); IR (KBr) 3420, 2923, 1586, 1564, 1501, 1472, 1433, 1413, 1366, 1145, 1001, 783, 741 cm^{-1}; ^1H NMR (400 MHz, $CDCl_3$) δ 2.94 (s, 6H) 7.21–7.22 (m, 1H) 7.23 (t, 1H) 7.74 (td, 1H) 7.79 (td, 1H) 8.12 (d, J = 8.24 Hz, 1H) 8.27 (d, J = 8.24 Hz, 1H) 8.53 (d, J = 4.58 Hz, 1H) 8.75 (d, 1H); ^{13}C NMR (400 MHz, $CDCl_3$) δ 46.41, 118.91, 121.13, 123.43, 123.51, 136.65, 136.79, 148.82, 149.21, 151.95, 154.11, 154.82, 157.13, 135.57; (EI) m/z 282 (M^+); HRMS (EI) calcd for $C_{15}H_{14}N_4S$, 282.0939; found, 282.0938.

2,4-Di(pyridin-2-yl)-*N*,*N*-di-*p*-tolylthiazol-5-amine (4b)

General procedure A. 4b (0.23 g, 76%) as a greenish yellow solid (mp: 171–172 °C); IR (KBr) 3053, 3021, 2917, 2856, 2359, 1882, 1784, 1505, 1292, 811 cm^{-1}; ^1H NMR (400 MHz, $CDCl_3$) δ 2.22 (s, 6H), 6.95–7.04 (m, 9H), 7.24–7.27 (m, 1H), 7.50 (td, 1H), 7.73–7.79 (m, 2H), 8.32–8.35 (m, 1H), 8.50–8.51 (m, 1H), 8.53–8.55 (m, 1H); ^{13}C NMR (500 MHz, $CDCl_3$) δ 20.8, 119.7, 112.1, 112.2, 122.7, 124.4, 129.8, 133.0, 136.1, 136.9, 144.7, 146.3, 147.5, 149.32, 149.39, 151.5, 151.8, 162.8; MS (EI) m/z 434 (M^+); HRMS (EI) calcd for $C_{27}H_{22}N_4S$, 434.1565; found, 434.1549.

2-(5-Methylpyridin-2-yl)-4-(pyridin-2-yl)-*N*,*N*-di-*p*-tolylthiazol-5-amine (4c)

General procedure A. 4c (0.077 g, 59%) as a yellow solid (mp: 116–117 °C); IR (KBr) 1686, 1605, 1383, 1314, 1287, 1002, 810 cm^{-1}; ^1H NMR (400 MHz, $CDCl_3$) δ 2.23 (s, 6H) 2.36 (s, 3H) 6.95–6.95 (m, 1H) 6.98 (m, 6H) 7.01 (t, 1H) 7.04–7.07 (m, 1H) 7.51–7.53 (m, 1H) 7.57 (dd, 1H) 7.78 (d, J = 7.79 Hz, 1H) 8.26–8.27 (m, 1H) 8.33 (d, J = 1.83 Hz, 1H) 8.58 (s, 1H); ^{13}C NMR (400 MHz, $CDCl_3$) δ 18.6, 20.8, 119.0, 119.2, 121.2, 122.1, 122.7, 129.7, 132.8, 134.4, 136.0, 137.3, 144.6, 149.1, 149.51, 149.6, 151.9, 161.8, 163.3; MS (EI) m/z 434 (M^+); HRMS (EI) calcd for $C_{28}H_{24}N_4S$, 448.1722; found, 448.1716.

2-Phenyl-4-(pyridin-2-yl)-*N*,*N*-di-*p*-tolylthiazol-5-amine (4d)

General procedure A. 4d (0.171 g, 59%) as a yellow solid (mp: 135–136 °C); IR (KBr) 3420, 1507, 1475, 1426, 1314, 1290, 814, 761, 686 cm^{-1}; ^1H NMR (400 MHz, $CDCl_3$) δ 2.29 (s, 6H), 7.03–7.05 (m, 4H), 7.07–7.09 (m, 4H), 7.42–7.45 (m, 2H), 7.47–7.48 (m, 2H), 8.02–8.03 (d, J = 3.7 Hz, 2H), 8.22 (d, J = 6.4, 2H), 9.09–9.10 (d, J = 3.7 Hz, 1H); ^{13}C NMR (400 MHz, $CDCl_3$) δ 20.8, 102.3, 118.1, 122.1, 122.4, 122.8, 126.6, 127.7, 128.8, 129.9, 130.2, 133.4, 144.4, 150.4, 156.3, 162.8; MS (EI) m/z 433 (M^+); HRMS (EI) calcd for $C_{28}H_{23}N_3S$, 433.1613; found, 433.1612.

N,*N*,2-Triphenyl-4-(pyridin-2-yl)thiazol-5-amine (4e)

General procedure A. 4e (0.064 g, 32%) as a yellow ocher solid (mp: 174–175 °C); IR (KBr) 2359, 2334, 1734, 1716, 1698, 1684, 1653, 1583, 1541, 1519, 1490, 1422, 1352, 1312, 1284, 1233, 846, 729, 757, 698 cm^{-1}; ^1H NMR (400 MHz, $CDCl_3$) δ 6.89 (t, 2H), 6.94–6.98 (m, 1H), 7.06–7.14 (m, 9H), 7.32–7.34 (m, 2H), 7.45 (td, 1H), 7.74 (d, J = 7.8, 1H), 7.89–7.92 (m, 2H), 8.42–8.44 (m, 1H) cm^{-1}; ^{13}C NMR (400 MHz, $CDCl_3$) δ 121.9, 122.1, 122.6, 123.0, 126.4, 128.7, 129.0, 120.0, 133.7, 135.9, 143.6, 146.6, 147.4, 149.4, 151.9, 163.0; MS (EI) m/z 433 (M^+); HRMS (EI) calcd for $C_{26}H_{19}N_3S$, 405.1300; found, 405.1281.

4-Phenyl-2-(pyridin-2-yl)-*N*,*N*-di-*p*-tolylthiazol-5-amine (4f)

General procedure A. 4f 4(0.0219 g, 90%) as a greenish yellow solid (mp: 192–193 °C); IR (KBr) 3421, 2921, 1586, 1569, 1506, 1470, 1424, 12 990, 1002, 811, 508 cm^{-1}; ^1H NMR (400 MHz, $CDCl_3$) δ 2.24 (s, 6H), 6.96–7.04 (m, 8H), 7.18–7.22 (tt, 1H), 7.24–7.25 (m, 1H), 7.26–7.28, (dd, 1H), 7.31–7.34 (td, 1H), 7.81–7.85 (td, 1H), 7.93–7.96 (dd, 2H), 8.29 (d, J = 7.79 Hz, 1H) 8.56 (d, J =

4.58 Hz, 1H); ^{13}C NMR (400 MHz, $CDCl_3$) δ 20.7, 119.6, 121.75, 124.4, 127.4, 127.9, 128.2, 129.8, 132.7, 133.5, 137.5, 143.8, 144.54, 148.4, 148.8, 151.2; MS (EI) m/z 433 (M^+); HRMS (EI) calcd for $C_{28}H_{23}N_3S$, 433.1613; found, 433.1621.

2-(4-Methoxyphenyl)-4-(pyridin-2-yl)-*N*-(*p*-tolyl)thiazol-5-amine (6a)

General procedure B. 6a (0.66 g, 60%) as a pale yellow solid (mp: 136 °C); IR (ATR) 2996, 1589, 1565, 1547, 1513, 1395, 1320, 1294, 1240, 1167, 1146, 1025, 971, 827, 782, 703, 493 cm^{-1}; ^{1}H NMR (400 MHz, $CDCl_3$) δ 2.33 (s, 3H), 3.84 (s, 3H) 6.93 (d, J = 8.53 Hz, 2H), 7.07–7.24 (m, 5H), 7.74 (t, 1H), 7.82–7.85 (m, 2H), 8.23 (s, 1H), 8.52 (d, J = 4.49 Hz, 1H), 11.5 (s, 1H); ^{13}C NMR (400 MHz, $CDCl_3$) δ 20.8, 55.4, 114.3, 117.8, 119.7, 120.8, 127.0, 130.0, 136.8, 139.9, 146.8, 147.1, 160.3; MS (EI) m/z 373(M^+); HRMS (EI) calcd for $C_{22}H_{19}N_3OS$, 373.1249; found, 373.1245.

N-(4-(*Tert*-butyl)phenyl)-2-(4-methoxyphenyl)-4-(pyridin-2-yl) thiazol-5-amine (6b)

General procedure B. 6b (0.42 g, 49%) as a pale-yellow solid (mp: 120 °C); IR (ATR) 2956, 1587, 1563, 1535, 1471, 1387, 1245, 1170, 1032, 825, 782, 705, 541, 513 cm^{-1}; ^{1}H NMR (400 MHz, $CDCl_3$) δ 1.35 (s, 9H), 3.83 (s, 3H) 6.93 (d, J = 8.98 Hz, 2H), 7.04–7.07 (m, 1H), 7.24–7.28 (m, 2H), 7.40 (d, J = 8.08 Hz, 2H), 7.72 (t, 1H), 7.84 (d, J = 8.53 Hz, 2H), 8.12–8.28 (m, 1H), 8.51 (d, J = 4.94 Hz, 1H), 11.6 (s, 1H); ^{13}C NMR (400 MHz, $CDCl_3$) δ 31.5, 34.0, 55.4, 111.9, 112.3, 114.3, 117.2, 117.3, 119.6, 120.7, 125.7, 126.3, 127.0, 130.3, 130.7, 136.6, 139.7, 145.0, 145.4, 147.1, 149.0, 155.8, 160.3; MS (EI) m/z 415(M^+); HRMS (EI) calcd for $C_{25}H_{25}N_3OS$, 415.1718; found, 415.1705.

Complex [Ni(4a)Cl] (7a)

General procedure C. 5a (0.0355 g, 86%) as a green solid (mp: 264–265 °C); IR (KBr) 3274, 1597, 1545, 1507, 1463, 1374, 1078, 786 cm^{-1}; ESI-MS calcd for $C_{15}H_{14}Cl_2N_4NiS$, 374.9981; found 375.8088.

Complex [Ni(4b)Cl] (7b)

General procedure C. 7b (0.05 g, 85%) (mp: 193–194 °C); IR (KBr) 3421, 2921, 2852, 1597, 1506, 1455, 1262, 811, 778, 676 cm^{-1}; ESI-MS calcd for $C_{27}H_{22}Cl_2N_4NiS$, 562.0607; found 562.0301.

Complex [Ni(4c)Cl] (7c)

General procedure C. 7c (0.024 g, 88%) (mp: 306–307 °C); IR (KBr) 3370, 1600, 1506, 1455, 1267, 813 cm^{-1}; ESI-MS calcd for $C_{28}H_{24}Cl_2N_4NiS$, 541.0764; found 542.2366.

Complex [Ni(4d)Cl] (7d)

General procedure C. 7d (0.066 g, 83%) (mp: 292–293 °C); IR (KBr) 3383, 2921, 1707, 1603, 1473, 1361, 1238, 813, 682, 566 cm^{-1}; ESI-MS calcd for $C_{56}H_{46}ClN_6NiS_2$, 959.2267; found 959.0425.

Complex [Ni(4e)Cl] (7e)

General procedure C. 7e (0.035 g, 97%) (mp: 177–178 °C); IR (KBr) 3384, 1602, 1489, 1360, 1237, 753, 694 cm^{-1}; ESI-MS calcd for $C_{52}H_{38}Cl_2N_6NiS_2$, 903.1641; found 903.0425.

Complex [Ni(4f)Cl] (7f)

General procedure C. 7f (0.05 g, 97%) (mp: 292–293 °C); IR (KBr) 3370, 1600, 1506, 1455, 1267, 813 cm^{-1}; ESI-MS calcd for $C_{56}H_{46}ClN_6NiS_2$, 959.2267; found 961.1050.

Complex [Zn(4f)$_2$Cl$_2$] (8a)

General procedure D. 8a (0.079 g, 93%) as a red solid (mp: 230–233 °C); IR (ATR) 1600, 1505, 1474, 1454, 1357, 1259, 811, 780, 753, 698, 501 cm^{-1}; ^{1}H NMR (500 MHz, $CDCl_3$) δ 2.25 (s, 6H), 6.90 (d, J = 8.53 Hz, 4H), 7.00 (d, J = 8.08 Hz, 4H), 7.26–7.26 (m, 3H) 7.63–7.66 (m, 1H), 7.69–7.71 (m, 1H), 7.74 (dd, 2H), 8.04 (td, 1H), 8.74 (d, J = 4.94 Hz, 1H); ^{13}C NMR (400 MHz, $CDCl_3$) δ 20.9, 25.6, 68.2, 121.5, 122.8, 126.9, 128.5, 128.8, 129.6, 129.8, 130.2, 134.8, 141.1, 143.3, 145.3, 145.6, 147.1, 148.8, 154.7; ESI-MS calcd for $C_{56}H_{46}ClN_6S_2Zn^+$, 965.2205; found 965.2498.

Complex [Zn(4f)$_2$Br$_2$] (8b)

General procedure D. 8b (0.072 g, 73%) as a yellow solid (mp: >250 °C); IR (ATR) 3027, 2969, 1738, 1602, 1539, 1506, 1476, 1455, 1364, 1228, 1216, 1011, 807, 776, 700, 556, 510, 408 cm^{-1}; ^{1}H NMR (500 MHz, $CDCl_3$) δ 2.25 (s, 6H), 6.90 (d, J = 8.53 Hz, 4H), 7.00 (d, J = 8.08 Hz, 4H), 7.26–7.26 (m, 3H) 7.63–7.66 (m, 1H), 7.69–7.71 (m, 1H), 7.74 (dd, 2H), 8.04 (td, 1H), 8.74 (d, J = 4.94 Hz, 1H); ^{13}C NMR (400 MHz, $CDCl_3$) δ 20.8, 121.5, 122.8, 126.9, 128.5, 128.8, 129.6, 129.8, 130.2, 134.8, 141.1, 143.3, 145.3, 145.6, 147.1, 148.8, 154.7; ESI-MS calcd for $C_{56}H_{46}BrN_6S_2Zn^+$, 1012.4300; found 1012.2454.

Complex [Zn(4f)$_2$I$_2$] (8c)

General procedure D. 8c (0.076 g, 67%) as a yellow solid (mp: >250 °C); IR (ATR) 3026, 2969, 1738, 1597, 1506, 1472, 1449, 1369, 1228, 1216, 1159, 1012, 810, 771, 700, 573, 513, 411 cm^{-1}; ^{1}H NMR (500 MHz, $CDCl_3$) δ 2.25 (s, 6H), 6.90 (d, J = 8.53 Hz, 4H), 7.00 (d, J = 8.08 Hz, 4H), 7.26–7.26 (m, 3H) 7.63–7.66 (m, 1H), 7.69–7.71 (m, 1H), 7.74 (dd, 2H), 8.04 (td, 1H), 8.74 (d, J = 4.94 Hz, 1H); ^{13}C NMR (400 MHz, $CDCl_3$) δ 20.8, 121.5, 122.8, 126.9, 128.5, 128.8, 129.6, 129.8, 130.2, 134.8, 141.1, 143.3, 145.3, 145.6, 147.1, 148.8, 154.7; ESI-MS calcd for $C_{56}H_{46}IN_6S_2Zn^+$, 1057.1562; found 1057.2929.

Author contributions

Khurnia Krisna Puji Pamungkas synthesized compounds, studied their photophysical properties and wrote the manuscript, Toshifumi Maruyama performed and determined X-ray structure, and Toshiaki Murai, supervised the project and wrote the manuscript.

Conflicts of interest

There are no conflicts to declare.

Acknowledgements

This research was partly supported by Koshiyama Science & Technology Foundation and a Grant-in-Aid for Scientific Research (B) (19H02712) and (C) (22K05109) from MEXT.

Notes and references

1 V. Ji Ram, A. Sethi, M. Nath and R. Pratap, in *The Chemistry of Heterocycles*, Elsevier, 2019, pp. 149–478.
2 P. C. Sharma, K. K. Bansal, A. Sharma, D. Sharma and A. Deep, *Eur. J. Med. Chem.*, 2020, **188**, 112016.
3 H. Liu, L. Xu, H. Hui, R. Vivian, C. Callebaut, B. P. Murray, A. Hong, M. S. Lee, L. K. Tsai, J. K. Chau, K. M. Stray, C. Cannizzaro, Y. C. Choi, G. R. Rhodes and M. C. Desai, *Bioorg. Med. Chem. Lett.*, 2014, **24**, 989–994.
4 M. R. Shreykar and N. Sekar, *Dyes Pigm.*, 2017, **142**, 121–125.
5 K. I. Lugovik, A. V. Popova, A. K. Eltyshev, E. Benassi and N. P. Belskaya, *Eur. J. Org. Chem.*, 2017, 4175–4187.
6 P. Gayathri, K. Kanagajothi, P. Nag, N. Anand, V. S. Reddy, D. Moon, S. P. Anthony and V. Madhu, *CrystEngComm*, 2021, **23**, 6769–6777.
7 P. O. Suntsova, A. K. Eltyshev, T. A. Pospelova, P. A. Slepukhin, E. Benassi and N. P. Belskaya, *Dyes Pigm.*, 2019, **166**, 60–71.
8 H. Sun, W.-H. Sun, Y. Jiang, J.-H. Wei, Y. Zhao, R. Zhang and Z.-H. Ni, *Dyes Pigm.*, 2020, **173**, 107938.
9 K. K. Puji Pamungkas, T. Maruyama and T. Murai, *Org. Biomol. Chem.*, 2021, **19**, 6804–6811.
10 M. A. Potopnyk, R. Lytvyn, Y. Danyliv, M. Ceborska, O. Bezvikonnyi, D. Volyniuk and J. V. Gražulevičius, *J. Org. Chem.*, 2018, **83**, 1095–1105.
11 J. R. Lakowicz, *Anal. Biochem.*, 2001, **298**, 1–24.
12 Y. Jeong, Y.-M. Kook, K. Lee and W.-G. Koh, *Biosens. Bioelectron.*, 2018, **111**, 102–116.
13 M. Abd El Aleem Ali Ali El-Remaily, T. El-Dabea, M. Alsawat, M. H. H. Mahmoud, A. Abdulaziz Alfi, N. El-Metwaly and A. M. Abu-Dief, *ACS Omega*, 2021, **6**, 21071–21086.
14 M. A. E. A. A. A. El-Remaily, A. M. M. Soliman, M. E. Khalifa, N. M. El-Metwaly, A. Alsoliemy, T. El-Dabea and A. M. Abu-Dief, *Appl. Organomet. Chem.*, 2022, **36**, e6320.
15 X. Zou, P. Shi, A. Feng, M. Mei and Y. Li, *Transition Met. Chem.*, 2021, **46**, 263–272.
16 X.-Z. Zou, A.-S. Feng, Y.-Z. Liao, X.-Y. Xu, H.-Y. Wen, A. You, M. Mei and Y. Li, *Inorg. Chem. Commun.*, 2020, **118**, 108030.
17 R. Menzel, S. Kupfer, R. Mede, D. Weiß, H. Görls, L. González and R. Beckert, *Eur. J. Org. Chem.*, 2012, 5231–5247.
18 S. E. Huffman, G. K. Yawson, S. S. Fisher, P. J. Bothwell, D. C. Platt, M. A. Jones, C. G. Hamaker and M. I. Webb, *Metallomics*, 2020, **12**, 491–503.
19 T. D. Thangadurai and S.-K. Ihm, *Synth. React. Inorg., Met.-Org., Nano-Met. Chem.*, 2005, **35**, 499–507.
20 Y. Liu, X. Sun, Y. Wang and Z. Wu, *Synth. Met.*, 2014, **198**, 67–75.
21 A. J. Hallett, E. Placet, R. Prieux, D. McCafferty, J. A. Platts, D. Lloyd, M. Isaacs, A. J. Hayes, S. J. Coles, M. B. Pitak, S. Marchant, S. N. Marriott, R. K. Allemann, A. Dervisi and I. A. Fallis, *Dalton Trans.*, 2018, **47**, 14241–14253.
22 H. Leopold, A. Tronnier, G. Wagenblast, I. Münster and T. Strassner, *Organometallics*, 2016, **35**, 959–971.
23 T. Y. Chikineva, D. S. Koshelev, A. V. Medved'ko, A. A. Vashchenko, L. S. Lepnev, A. S. Goloveshkin and V. V. Utochnikova, *Russ. J. Inorg. Chem.*, 2021, **66**, 170–178.
24 N. Dannenbauer, P. R. Matthes, T. P. Scheller, J. Nitsch, S. H. Zottnick, M. S. Gernert, A. Steffen, C. Lambert and K. Müller-Buschbaum, *Inorg. Chem.*, 2016, **55**, 7396–7406.
25 L. Luconi, D. M. Lyubov, A. Rossin, T. A. Glukhova, A. V. Cherkasov, G. Tuci, G. K. Fukin, A. A. Trifonov and G. Giambastiani, *Organometallics*, 2014, **33**, 7125–7134.
26 L. A. Büldt, C. B. Larsen and O. S. Wenger, *Chem.–Eur. J.*, 2017, **23**, 8541.
27 C. Núñez, R. Bastida, A. Macías, L. Valencia, J. Ribas, J. L. Capelo and C. Lodeiro, *Dalton Trans.*, 2010, **39**, 7673–7683.
28 N. Meundaeng, A. Rujiwatra and T. J. Prior, *Transition Met. Chem.*, 2016, **41**, 783–793.
29 A. Rossin, B. Di Credico, G. Giambastiani, L. Gonsalvi, M. Peruzzini and G. Reginato, *Eur. J. Inorg. Chem.*, 2011, **2**, 539–548.
30 A. Helal and H. S. Kim, *Tetrahedron*, 2010, **66**, 7097–7103.
31 E. Ergun, Ü. Ergun, Ö. İleri and M. F. Küçükmüzevir, *Spectrochim. Acta, Part A*, 2018, **203**, 273–286.
32 Y. Mikata, A. Takekoshi, M. Kaneda, H. Konno, K. Yasuda, M. Aoyama and S. Tamotsu, *Dalton Trans.*, 2017, **46**, 632–637.
33 P. K. Mehta, E. T. Oh, H. J. Park and K. H. Lee, *Spectrochim. Acta, Part B*, 2017, **245**, 996–1003.
34 F. Yu, X. Guo, X. Tian and L. Jia, *J. Fluoresc.*, 2017, **27**, 723–728.
35 J. Y. Yun, A. Kim, S. M. Hwang, D. Yun, H. Lee, K.-T. Kim and C. Kim, *Bull. Chem. Soc. Jpn.*, 2019, **92**, 961–966.
36 D. Aydin, S. N. Karuk Elmas, T. Savran, F. N. Arslan, G. Sadi and I. Yilmaz, *J. Photochem. Photobiol., A*, 2021, **419**, 113459.
37 Y. Watanabe, W. Sungnoi, A. O. Sartorio, M. Zeller and A. Wei, *Mater. Chem. Front.*, 2020, **4**, 899–904.
38 K. Yamaguchi, T. Murai, S. Hasegawa, Y. Miwa, S. Kutsumizu, T. Maruyama, T. Sasamori and N. Tokitoh, *J. Org. Chem.*, 2015, **80**, 10742–10756.
39 K. Yamaguchi, T. Murai, J. D. Guo, T. Sasamori and N. Tokitoh, *ChemistryOpen*, 2016, **5**, 396.
40 K. Yamaguchi, T. Murai, Y. Tsuchiya, Y. Miwa, S. Kutsumizu, T. Sasamori and N. Tokitoh, *RSC Adv.*, 2017, **7**, 18132–18135.
41 T. Murai, H. Furukawa and K. Yamaguchi, *Heterocycles*, 2018, **97**, 409–421.
42 T. Murai, M. Yoshihara, K. Yamaguchi and M. Minoura, *Asian J. Org. Chem.*, 2019, **8**, 1102–1106.
43 T. Murai, Y. Nakatsu, Y. Tsuchiya, K. Yamaguchi, T. Maruyama, Y. Miwa and S. Kutsumizu, *Heterocycles*, 2020, **101**, 611–620.
44 Y. Tsuchiya, K. Yamaguchi, Y. Miwa, S. Kutsumizu, M. Minoura and T. Murai, *Bull. Chem. Soc. Jpn.*, 2020, **93**, 927–935.